

Hadronic gamma-ray emission from Cygnus OB2

S. Menchiari,^{a,*} G. Morlino,^b E. Amato^b and N. Bucciantini^b

^aUniversità degli Studi di Siena,
Via Roma 56 - 53100, Siena, Italy

^bINAF, Osservatorio Astrofisico di Arcetri,
L.go E. Fermi 5, Firenze, Italy

E-mail: menchiari2@student.unisi.it

In the last decade, the detection by diverse experiments of diffuse gamma-ray emissions toward several Galactic young massive star clusters has renewed attention to these objects as potential Galactic cosmic ray accelerators. Indeed, the conversion of a few percent of the power supplied by the strong winds from the massive stars into accelerated particles is enough to explain the observed gamma-ray luminosities in a purely hadronic scenario. Cygnus OB2 is one of the massive star clusters found in coincidence with diffuse gamma-ray emission detected in a broad range of energies, from a few GeV up to 1.4 PeV.

In this work, we aim to compare the morphology and spectrum of the observed gamma emission with those predicted from a theoretical model where particles are accelerated at the termination shock of the cluster wind. The expected properties of the γ -ray emission depend on the distribution of accelerated cosmic rays, which is determined by the physics of acceleration at the termination shock and propagation in the hot expanding bubble created by the cluster wind. Propagation and acceleration are in turn strongly linked to the type of turbulence spectrum in the hot plasma filling the bubble.

After testing different turbulence spectra, we found that our model **can well reproduce the spectral energy distribution assuming a diffusion either Kraichnan- or Bohm-like**. The predicted radial profile agrees well with HAWC observations but not with Fermi results. According to our best fit model, Cygnus OB2 should be able to accelerate cosmic rays up to 1 PeV, and would hence be a PeVatron.

*7th Heidelberg International Symposium on High-Energy Gamma-Ray Astronomy (Gamma2022)
4-8 July 2022
Barcelona, Spain*

*Speaker

1. Introduction

Young massive star clusters (YMSCs) are considered a potential new class of Galactic cosmic ray (CR) accelerators [5]. The detection of diffuse γ -ray emission in coincidence with several of these objects, such as Cygnus OB2 [2, 3], Westerlund 1 [6], and Westerlund 2 [20], has provided strong evidence for the presence of freshly accelerated CRs in these sources. The energy for non-thermal activity is thought to be supplied by the powerful winds blown by the hundreds of massive stars hosted in the cluster core. Several scenarios for particle acceleration have been proposed: shocks caused by wind-wind collisions [8], winds of Wolf-Rayet stars [12] or the termination shock (TS) of the collective wind resulting from the sum of individual stellar winds [14].

On a general ground, it is possible to investigate the properties of YMSCs as CR accelerators through a comprehensive morphological and spectral analysis of the diffuse γ -ray emission generated by the population of freshly injected CRs. In this work, we will focus on the scientific case of the YMSC Cygnus OB2 and derive its properties as a CR accelerator through comparison of its gamma-ray emission with predictions based on the model of acceleration at the cluster wind TS developed by [14]. One of the key outcomes of the paper of [14] is that the spectral and morphological properties of the CR distribution near YMSCs are strongly affected by the type of plasma turbulence in the system. In fact, different types of turbulent cascade will reflect in different spectra of injected CRs. In addition, the propagation physics from the acceleration site will also be affected, yielding different morphological shapes in the downstream region. If one assumes a pure hadronic scenario, the spectro-morphological properties of the γ -ray emission can be potentially used to distinguish between the various turbulence models. From there, it is then possible to infer the properties of the accelerator, such as, for example, the maximum energy of the accelerated particles.

2. Cosmic ray distribution in the vicinity of a young massive star cluster

The collective interaction of the powerful winds from a YMSC can excavate a cavity inside the interstellar medium (ISM). This wind cavity is composed of an inner region, upstream of the TS, and an outer region downstream of the TS. The latter is filled with shocked wind material in adiabatic expansion in the ISM. The radius of the wind TS, R_{TS} and of the expanding forward shock, R_b , can be estimated as [18]: $R_{\text{TS}} = 0.7 \times L_w^{-1/5} \dot{M}^{1/2} u_1^{1/2} \rho_H^{-3/10} t_{\text{age}}^{2/5}$ and $R_b = 0.76 \times (L_w/\rho_H)^{1/5} t_{\text{age}}^{3/5}$, where L_w and u_1 are the wind luminosity and speed respectively, \dot{M} and t_{age} are the cluster mass loss rate and age, and ρ_H is the ISM density in the cluster surroundings. For Cygnus OB2 $t_{\text{age}} = 3$ Myr [19] and we assume $\rho_H = 10 m_p \text{ cm}^{-3}$. Knowing the Cygnus OB2 star population [19], one can estimate $L_w = \sum_i \dot{M}_i v_{\infty,i}^2 / 2$ and $\dot{M} = \sum_i \dot{M}_i$, where the index i refers to the i -th star of the cluster and $v_{\infty,i}$ is the single star wind terminal velocity [13]. The mass loss rates of individual stars, \dot{M}_i , are calculated using eq. A.1 of [15]. Taking into account the uncertainties in the stellar parameters, we estimate $L_w \sim (1.5 - 5) \times 10^{38} \text{ erg s}^{-1}$ and $\dot{M} \sim (0.85 - 2) \times 10^{-4} \text{ M}_{\odot} \text{ yr}^{-1}$. Using the mean values $L_w = 2 \times 10^{38} \text{ erg s}^{-1}$ and $\dot{M} = 10^{-4} \text{ M}_{\odot} \text{ yr}^{-1}$, we find: $R_{\text{TS}} \simeq 16 \text{ pc}$, $R_b \simeq 86 \text{ pc}$, and $u_1 = \sqrt{2L_w/\dot{M}} \sim 2500 \text{ km s}^{-1}$.

For the CR distribution, $f_{\text{CR}}(E, r)$, we use the steady state spherical model developed by [14], in which particles are accelerated at the TS and then escape from the system through a combination of advection and diffusion. The CR distribution upstream (f_1) and downstream (f_2) of the TS, an

in the region outside the bubble (f_{ISM}) are:

$$\begin{aligned}
 f_1(r < R_{\text{TS}}, E) &\simeq f_{\text{TS}}(E) \exp[-u_1(R_{\text{TS}} - r)/D_1(E)] \\
 f_2(R_{\text{TS}} < r < R_b, E) &= f_{\text{TS}}(E) e^{\alpha(r)} \frac{1 + \beta[e^{\alpha(R_b)} e^{-\alpha(r)} - 1]}{1 + \beta[e^{\alpha(R_b)} - 1]} + f_{\text{gal}}(E) \frac{\beta[e^{\alpha(r)} - 1]}{1 + \beta[e^{\alpha(R_b)} - 1]} \quad (1) \\
 f_{\text{ISM}}(r > R_b, E) &= f_2(R_b, E) (R_b/r) + f_{\text{gal}}(E) (1 - R_b/r)
 \end{aligned}$$

where $\alpha(r) = u_2 R_{\text{TS}}(1 - R_{\text{TS}}/r)/D_2(E)$, $\beta(E) = [D_{\text{ISM}}(E)R_b]/(u_2 R_{\text{TS}}^2)$. Eq.(1) is a first order approximation to the full solution presented in [14] but it is adequate for the aims of the present work. The subscripts 1 and 2 refer to regions upstream and downstream of the TS, respectively. The wind speed is constant in the upstream, $u = u_1$, while downstream of the TS $u = u_2(r/R_{\text{TS}})^{-2}$ with $u_2 = u_1/4$ (for strong shocks). D is the diffusion coefficient in the system, which depends on the type of plasma turbulence. We here consider three possible turbulence spectra: Kolmogorov-like, Kraichnan-like and flat spectrum (Bohm-like). The corresponding diffusion coefficients are: $D_{\text{K41}}(E) = \frac{1}{3}\beta c r_L^{1/3} L_c^{2/3}$, $D_{\text{Kra}}(E) = \frac{1}{3}\beta c r_L^{1/2} L_c^{1/2}$ and $D_{\text{Bohm}}(E) = \frac{1}{3}\beta c r_L$, where β is the particles speed normalized to the speed of light, c , and $r_L = p c/eB$ is the Larmor radius, with p the particle momentum and B the magnetic field. To calculate B , we assume that a fraction η_B of the wind luminosity is converted into turbulent magnetic field. The other 2 quantities that appear in Eq.(1) are f_{gal} , the distribution of the Galactic CR sea - as inferred, e.g., from AMS-02 data [4] - and f_{TS} , the distribution of accelerated particles at the TS. The general solution for f_{TS} is quite involved [see 14], and depends on the type of diffusion coefficient. We here use an approximation to the formal expression:

$$f_{\text{TS}}(p) = \frac{6n_1 u_1^2 \epsilon_{\text{CR}}}{8\pi \Lambda_p (m_p c)^3 c^2} \left(\frac{p}{m_p c}\right)^{-s} \left[1 + a_1 \left(\frac{p}{p_{\text{max}}}\right)^{a_2}\right] e^{-a_3 (p/p_{\text{max}})^{a_4}} \quad (2)$$

where n_1 is the particle density in the upstream, s the power-law index, ϵ_{CR} the fraction of wind luminosity converted in CRs, and $\Lambda_p = \int_{x_{\text{inj}}}^{\infty} x^2 f_{\text{TS}}(x) (\sqrt{1+x^2} - 1) dx$, with $x = p/m_p c$ and $x_{\text{inj}} = 1.7$. The coefficients a_i depend on the turbulence properties and are $a_1 = [10, 5, 8.94]$, $a_2 = [0.3, 0.45, 1.3]$, $a_3 = [22, 12.5, 5.3]$ and $a_4 = [0.4, 0.64, 1.13]$ for the Kolmogorov, Kraichnan and Bohm cases respectively. Finally, p_{max} is the maximum particle momentum achievable in the system, which depends again on the properties of local plasma turbulence. The maximum particle energy, $E_{\text{max}} = c p_{\text{max}}$, can be estimated by equating the particle diffusion length with R_{TS} : $D_1(E_{\text{max}})/u_1 = R_{\text{TS}}$,

3. Modeling the hadronic γ -ray emission

Once the CR distribution is known, the hadronic γ -ray flux from a region of volume V can be computed as:

$$\phi_{\gamma}(E_{\gamma}) = \frac{1}{4\pi d^2} \iint c f_{\text{CR}}(E_p, r) n(r) \frac{d\sigma(E_p, E_{\gamma})}{dE_p} dE_p dV, \quad (3)$$

where d is the distance of the source, σ is the cross-section for p-p interactions leading to π_0 -decay γ -rays [11], and E_p and E_{γ} are the CR and γ -ray energy respectively. In our case, $f_{\text{CR}}(E_p, r)$ is the radial distribution of CRs from section 2, while $n(r)$ is the distribution of target density close

to Cygnus OB2, which is largely unknown. We model the ISM as a combination of neutral (HI) and molecular (H₂) hydrogen. We use high-resolution 21 cm line data from the Canadian Galactic Plane survey to trace the amount of HI in the region [17]. To estimate the column density, we follow the same approach adopted in [5]. For the molecular component, we use, when available, a combination of high and low-resolution ¹²CO observations, from the Nobeyama radio telescope [16] and from the composite Galactic survey of [9], respectively. We then calculate the H₂ column density assuming a constant conversion factor $X_{\text{CO}} = 1.68 \cdot 10^{20} \text{ mol. cm}^{-2} \text{ km}^{-1} \text{ s K}^{-1}$ [3]. All observations are kinematically truncated between $\pm 20 \text{ km s}^{-1}$, in order to eliminate the contribution of gas from the Perseus and Outer arms. Finally, to obtain the volumetric density $n(r)$ we assume that the ISM is uniformly distributed along the line of sight on a scale of $\pm 400 \text{ pc}$ around the position of Cygnus OB2. The total extent of 800 pc is compatible with the distribution of dust towards the Cygnus-X star forming complex [10].

4. Comparison with data

To test which model parameters, if any, best reproduce the properties of Cygnus OB2, we compared the γ -ray emission computed in §3 with archival data from several instruments. In order to do so, we first find, through χ^2 minimization, the values of L_w , ϵ_{CR} and s that allow us to best fit the observed γ -ray spectral energy distribution (SED). All these parameters enter the CR distribution at the TS (Eq. 2), and L_w , in particular, affects both the normalization and the E_{max} . To fit the SED, we extract the γ -ray flux from a region of 2.2° centered on the stellar cluster (corresponding to a projected radius of $\sim 54 \text{ pc}$). When calculating the γ -ray emission, we set $f_{\text{gal}} = 0$, as in principle, the background contribution of the Galactic CRs is subtracted from the data. The SED data points considered for the procedure are the ones obtained by Fermi-LAT in the 4FGL (4FGL J2028.6+4110e) [1], by Argo (ARGO J2031+4157)[7], and by HAWC (HAWC J2030+409) [2]. All the measured fluxes are rescaled so as to refer them to the same size of the emission region, set to 2.2° . This is done by considering that in all cases, the emission is modeled using a 2D symmetric Gaussian profile with different widths: 2.0° for 4FGL J2028.6+4110e, 1.8° for ARGO J2031+4157 and 2.13° for HAWC J2030+409. When compared with the 2.2° we chose, these translate in scale factors: 0.45, 0.53 and 0.41. After constraining the spectral parameters, we consider the morphology and compare with Fermi-LAT [5] and HAWC [2] data the radial profile calculated in four rings centered on Cygnus OB2 (intervals in pc: [0–15], [15–29], [29–44], and [44–54]).

5. Results and conclusions

The result of the spectral fitting is shown in Table 1. All models can adequately fit the observed SED (see Fig. 1), and, from the point of view of pure statistics, the difference in χ^2 is not sufficient to define a preferred model. However, in the case of Kolmogorov turbulence, the wind luminosity required to fit the observed SED is more than a factor 10 higher than what estimated from the population of Cygnus OB2 stars. In order to fit the cut-off region, a high turbulence level is required. The latter is related to the wind luminosity through $\eta_B < 1$, but even for the unrealistically large value of $\eta_B = 0.9$ (see Fig. 1), $L_w > 10^{39} \text{ erg/s}$ is required. For these reasons, we conclude

that Kolmogorov turbulence is likely inadequate to describe the system. For Kraichnan turbulence, instead, the required L_w is only a factor ~ 2 higher than the estimate based on the population of Cygnus OB2 stars, $L_{w,*}$. Given the large uncertainties of this estimate, the discrepancy does not exclude the model. At odds with the former cases, Bohm turbulence, highly efficient at scattering particles, requires L_w a factor 10 lower than $L_{w,*}$. We then performed a new fit with $L_w = L_{w,*}$ and varying η_B . The results are reported in the last row of Table 1. For the second part of the

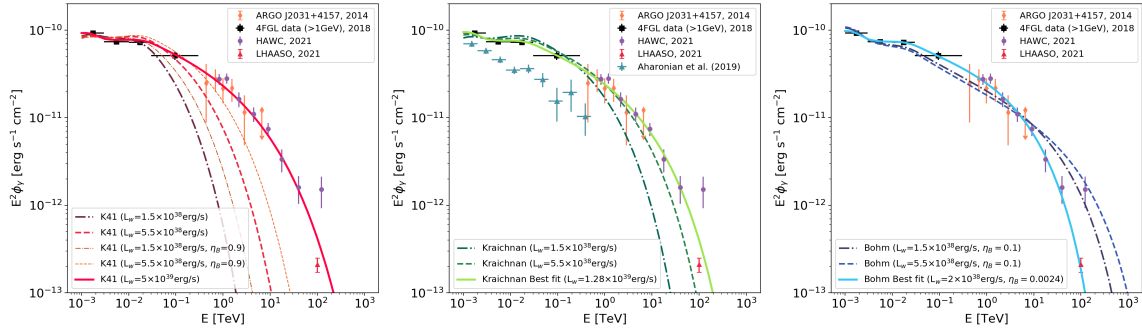


Figure 1: Spectral energy distribution of the expected hadronic γ -ray emission extracted from a region of 2.2° centered on Cyg OB2. The three panels refer to different turbulence models: Kolmogorov (left), Kraichnan (center) and Bohm (right). Solid lines are the best fit models, corresponding to parameters reported in Table 1. Other line types, as specified in each panel, are for SED calculated using fixed values of L_w corresponding to the minimum and maximum luminosity estimated in §2. Data points are from Fermi, HAWC, ARGO and LHAASO.

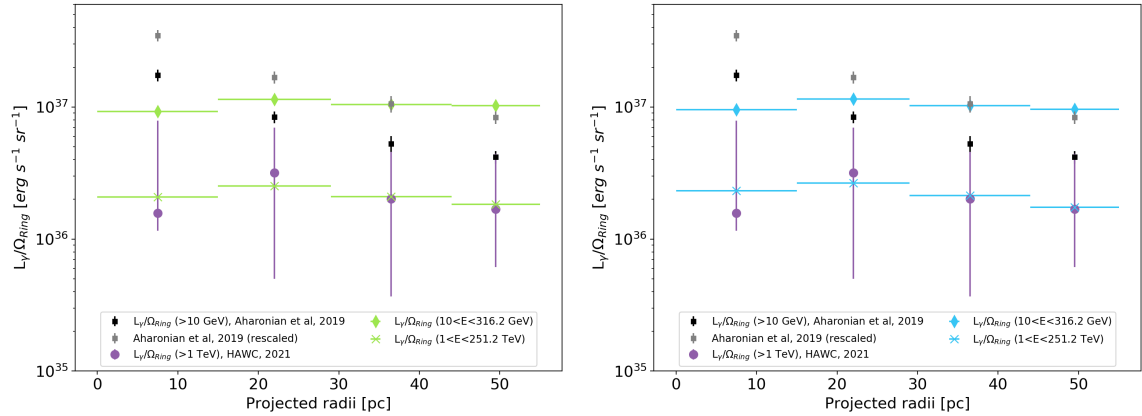


Figure 2: Comparison with observations of the expected radial profile of γ -ray surface brightness, for Kraichnan (left) and Bohm turbulence (right). Black squares are Fermi-LAT data [5], while purple circles are data from HAWC [2]. Grey squares represent Fermi-LAT measurements rescaled by a factor of 2. Diamonds and crosses represent the model predicted surface brightness at energies of $10 < E_\gamma < 316.2$ GeV and $1 < E_\gamma < 251.2$ TeV respectively.

study, focused on morphology, we only consider the turbulence models that allow us to reproduce the spectrum, namely Kraichnan and Bohm turbulence. Fig. 2 shows the comparison between the observed γ -ray radial profile and the prediction based on our best fit models. One can clearly see that the expected profile is compatible, in both the cases, with constant surface brightness. This

behaviour is a result of advection, dominating CR transport and making their distribution spatially constant. This trend is consistent with HAWC observations, but not with the radial morphology observed by Fermi-LAT, which shows a centrally peaked profile. The origin of the discrepancy is currently being investigated.

Models	L_w [erg s ⁻¹]	s	ϵ_{CR}	η_B	E_{max} [PeV]	R_{TS} [pc]	R_b [pc]	$\bar{\chi}^2$
Kolmogorov	$5 \cdot 10^{39}$	4.17	$4 \cdot 10^{-3}$	0.1	23	16	163	0.66
Kraichnan	$1.28 \cdot 10^{39}$	4.23	$7 \cdot 10^{-3}$	0.1	3.97	14	124	0.39
Bohm ^a	$1.9 \cdot 10^{37}$	4.27	$1.3 \cdot 10^{-1}$	0.1	0.51	12	53	0.27
Bohm ^b	$2 \cdot 10^{38}$	4.27	$2 \cdot 10^{-2}$	$2.4 \cdot 10^{-3}$	0.47	13	86	0.25

Table 1: Best fit parameters and main system characteristics of the resulting best fit model. For the Kolmogorov and Kraichnan case, the parameters varied during the fit are L_w , s, and ϵ_{CR} . For the Bohm model we separately show the two cases where we fit L_w , s, and ϵ_{CR} (case *a*) and η_B , s, and ϵ_{CR} (case *b*).

In summary, we have shown that the γ -ray emission from Cygnus OB2 can be adequately explained assuming that CRs are accelerated at the wind TS according to the model by [14]. For Kraichnan or Bohm turbulence the model well accounts for the source spectrum, and for the very-high-energy gamma-ray morphology. The inconsistency with Fermi-LAT data is under analysis. An interesting possibility is that the central peak is due to a population of leptons close to the TS.

References

- [1] Abdollahi S., et al., 2020, , 247, 33
- [2] Abeysekera A. U., et al., 2021, *Nature Astronomy*, 5, 465
- [3] Ackermann M., et al., 2011, *Science*, 334, 1103
- [4] Aguilar M., et al., 2015, *PRL*, 114, 171103
- [5] Aharonian F., Yang R., de Oña Wilhelmi E., 2019, *Nature Astronomy*, 3, 561
- [6] Aharonian F., et al., 2022, arXiv e-prints, p. arXiv:2207.10921
- [7] Bartoli B., et al., 2014, *The Astrophysical Journal*, 790, 152
- [8] Bykov A. M., Marcowith A., Amato E., Kalyashova M. E., Kruijssen J. M. D., Waxman E., 2020, , 216, 42
- [9] Dame T. M., Hartmann D., Thaddeus P., 2001, *The Astrophysical Journal*, 547, 792
- [10] Green G. M., Schlaflly E., Zucker C., Speagle J. S., Finkbeiner D., 2019, , 887, 93
- [11] Kafexhiu E., Aharonian F., Taylor A. M., Vila G. S., 2014, *Physical Review D*, 90, 123014
- [12] Kalyashova M. E., Bykov A. M., Osipov S. M., Ellison D. C., Badmaev D. V., 2019, in *Journal of Physics Conference Series*, p. 022011 (arXiv:1910.08602), doi:10.1088/1742-6596/1400/2/022011
- [13] Kudritzki R.-P., Puls J., 2000, , 38, 613
- [14] Morlino G., Blasi P., Peretti E., Cristofari P., 2021, *MNRAS*, 504, 6096
- [15] Renzo M., Ott C. D., Shore S. N., de Mink S. E., 2017, , 603, A118
- [16] Takekoshi T., et al., 2019, *The Astrophysical Journal*, 883, 156
- [17] Taylor A. R., et al., 2003, 125, 20
- [18] Weaver R., McCray R., Castor J., Shapiro P., Moore R., 1977, , 218, 377
- [19] Wright N. J., Drake J. J., Drew J. E., Vink J. S., 2010, , 713, 871
- [20] Yang R.-z., de Oña Wilhelmi E., Aharonian F., 2018, *Astronomy & Astrophysics*, 611, A77